Inhibition of Jahn–Teller Cooperative Distortion in LiMn2O4 Spinel by Transition Metal Doping

ARTICLE *in* PHYSICAL CHEMISTRY CHEMICAL PHYSICS · JANUARY 2001

Impact Factor: 4.49 · DOI: 10.1039/b100080m

7 AUTHORS, INCLUDING:

Marcella Bini
University of Pavia
76 PUBLICATIONS **1,262** CITATIONS
SEE PROFILE

V. Massarotti
University of Pavia
116 PUBLICATIONS **1,525** CITATIONS
SEE PROFILE

M. C. Mozzati
University of Pavia
134 PUBLICATIONS **1,322** CITATIONS
SEE PROFILE

PCCP

Inhibition of Jahn–Teller cooperative distortion in $LiMn_2O_4$ spinel by transition metal ion doping

Doretta Capsoni,[a] Marcella Bini,[a] Gaetano Chiodelli,[a] Vincenzo Massarotti,*[a] Carlo B. Azzoni,[b] Maria Cristina Mozzati[b] and Alberto Comin[b]

[a] *Dipartimento di Chimica Fisica and CSTE-CNR, Università di Pavia, via Taramelli 16, I-27100 Pavia, Italy. E-mail: vimas@chifis.unipv.it*

[b] *INFM-Dipartimento di Fisica "Alessandro Volta", Università di Pavia, via Bassi 6, I-27100 Pavia, Italy*

Received 2nd January 2001, Accepted 6th April 2001
First published as an Advance Article on the web 10th May 2001

The aim of this study is to determine the minimum amount of dopant that prevents the occurrence, near room temperature, of a Jahn–Teller (J–T) transition in the M-doped lithium manganese spinel of composition $Li_{1.02}M_xMn_{1.98-x}O_4$ with $0.00 < x \leqslant 0.06$ and M = Ni^{2+}, Co^{3+}, Cr^{3+} or Ti^{4+}. EPR spectra and magnetic susceptibility data are related to the valence state of M and Mn, and the homogeneous distribution of the dopant. We find that the spinel framework is remarkably sensitive to displaying low electronic and magnetic changes in its cationic sublattice due to cation substitution. The J–T distortion, which is associated with a sudden drop in conductivity with decreasing temperature, is suppressed by substituting 3% of Mn with Co^{3+} or Cr^{3+}, or by adding an even smaller amount of Ni^{2+} ($x = 0.02$, or 1% substitution). However, this inhibition occurs only in samples with a ratio $r = [Mn^{4+}]/[Mn^{3+}] \geqslant 1.18$, *i.e.*, a value larger than the ratio $r = 1.106$ we have with no doping ($x = 0$). As a consequence, doping with the tetravalent cation Ti^{4+}, which always decreases the r value, does not suppress the J–T transition. We suggest that both the dopant ion and the Li^+ in excess over the stoichiometric composition are located in 16d sites. The removal of the J–T transition in the Co^{3+} ($x = 0.06$) sample is also due to local disorder.

1. Introduction

Rechargeable lithium batteries now find a broad range of uses, in electrical vehicles as well as in microelectronic devices, thanks to their high energy density and environmental friendliness. The most popular cathode material is the lithium manganese oxide, $LiMn_2O_4$,[1,2] with a spinel structure containing unoccupied tetrahedral and octahedral sites which are suitable for insertion of lithium ions. The discharge/charge of a battery is due to the filling/emptying of these sites. Near room temperature (r.t.), the stoichiometric $LiMn_2O_4$ goes through a cubic-to-orthorhombic transition,[3,4] which is caused by a Jahn–Teller (J–T) cooperative distortion of the $Mn^{3+}O_6$ octahedra. Correspondingly, the Mn^{3+} sites switch from cubic to tetragonal symmetry, and the lithium insertion capacity is decreased. For this reason, we need to suppress the Jahn–Teller transition to achieve a long battery life and good performances at r.t.

It is well known[5] that the electrochemical properties of the lithium manganese spinel are related to the presence of both Mn^{3+} and Mn^{4+} ions, and to the possibility of increasing the ratio $r = [Mn^{4+}]/[Mn^{3+}]$ by adding an excess of lithium (y) according to the general formula $Li[Li_yMn_{2-y}]O_4$. Notice that, for the stoichiometric composition ($y = 0$), we have $r = 1$. X-Ray diffraction (XRD), EPR and magnetic susceptibility data[6] suggest the excess lithium ($y > 0$) is found in octahedral sites, $[Li]_{tetra}[Li_yMn_{1-3y}{}^{3+}\ Mn_{1+2y}{}^{4+}]_{octa}O_4$ while the structure of the lithium-poor compounds ($y < 0$) is $[Li_{1-|y|}Mn_{|y|}{}^{2+}]_{tetra}[Mn_{1+|y|}{}^{3+}Mn_{1-|y|}{}^{4+}]_{octa}O_4$.

For a very small excess of lithium, the J–T transition temperature is found below the transition point of the stoichiometric compound (280 K).[7,8] Furthermore, the structural changes accompanying the J–T transition are no longer observed above $y \sim 0.035$.

Doping with cations substituted into the 16d-spinel site provides another way of suppressing the J–T distortion. Substitution of Mn with Ti, Cr, Co, Ni, Ga or Zn may achieve stabilization of the spinel lattice.[9–20] In particular, the replacement of a Ni^{2+} ion at the Mn sites, as recently confirmed by neutron diffraction,[14] implies oxidation of Mn^{3+} to Mn^{4+}, and an increase in r.

In this paper, we study the lithium–manganese oxides doped with transition metal cations (Ni^{2+}, Co^{3+}, Cr^{3+} and Ti^{4+}). XRD, EPR and magnetic susceptibility measurements test the homogeneous dilution of the doping ions and the valence state of manganese; on the other hand, conductivity measurements as a function of temperature provide a sensitive test for the presence (or disappearance) of the J–T distortion. Our main goal is to prevent the J–T transition with the minimum amount of ionic substitution relative to the stoichiometry, in order to improve both the capacity and the lifetime of the Li–Mn battery.

2. Experimental

2.1. Materials and samples preparation

The lithium–manganese samples have been prepared by solid state reaction of MnO (Alfa, 99.9%) and Li_2CO_3 (Carlo Erba, R.P.) with a small lithium excess ($y = 0.016$). The doped samples have been obtained by adding transition metal oxides (CoO, NiO, Cr_2O_3 or TiO_2) in the amount required to obtain the composition $Li_{1.02}M_xMn_{1.98-x}O_4$ with $0.00 < x \leqslant 0.06$. The reactants were initially fired at 1073 K (in air for 2 h) to

 DOI: 10.1039/b100080m

decompose the carbonate, then brought to r.t. and ground. The sample was then heated back to 1073 K, at 5 K min^{-1}, and annealed for 8 h. The grinding–annealing cycle was repeated if X-ray checks revealed the presence of traces of the reactants or intermediate phases. Furthermore, EPR data were collected to determine the degree of inhomogeneity in the dopant distribution. For conductivity measurements, the powder was pressed in the form of bars and sintered at 1073 K in air for 10 h.

2.2. Apparatus and procedures

The X-ray powder diffraction patterns were collected with a Bruker D5005 diffractometer (Cu-Kα radiation, Bragg–Brentano geometry) equipped with a θ–θ goniometer and curved graphite monochromator on the diffracted beam. The patterns were collected in the $15 \leqslant 2\theta/\text{degrees} \leqslant 130$ angular range, with steps of 0.02° and 8 s counting time per step. The structural and profile (Rietveld method) analyses were performed with the FULLPROF program.[21]

EPR spectra in the X band (~9.3 GHz) over the temperature range 300–900 K were acquired with a Bruker spectrometer, and analyzed with suitable software. A continuous nitrogen flow apparatus was used to study temperature dependence. Static magnetization was measured from 300 down to 2 K with a SQUID magnetometer (Quantum Design). The system for conductivity measurements has been described elsewhere.[5]

3. Results

3.1. XRD

The r.t. diffraction patterns of the doped samples with $x = 0.02$ are very similar to the non-doped one, and display only the cubic spinel phase. The peak positions differ slightly depending on the Mn-substituted transition metal ions and agree quite well with those of the pure spinel. The broadening and angular position of the peaks increase with the doping ion content as shown in Fig. 1a and 1b for Cr and Co samples respectively (see inset). Fig. 2 plots the lattice parameter a (as obtained through Rietveld refinement) and shows that a decreases as x increases.

3.2. DC conductivity

The DC conductivity (σ) of the $x = 0.02$ samples are compared with that of the $x = 0$ sample in Fig. 3. The step in conductivity observed near r.t. in the $x = 0$ sample is due to the cubic–orthorhombic J–T transition.[3,4] Notice that Ti doping makes the transition sharper and increases its temperature. Ti is quite ineffective in removing the transition while Cr, Co and Ni cause an increase in conductivity at r.t. and a partial (for Cr and Co) or complete (for Ni) disappearance of the transition.

Fig. 4 shows the conductivity *vs.* T behavior for different contents of Cr (a) and Co (b). The sharp increase in the σ *vs.* T slope which marks the transition for $x < 0.02$, gradually disappears for higher dopant content and is no longer observed for $x = 0.06$.

3.3. EPR

The EPR signals of the samples at 300 K are reported in Fig. 5. A broad peak (feature A), characteristic of the stoichiometric compound, is present in all the samples. A sharper feature near 2000 G (feature B) is particularly evident in the $x_{Ti} = 0.02$, $x_{Co} = 0.02$ and $x_{Co} = 0.06$ samples: this feature shifts to 3400 G ($g \approx 2$) with increasing T (see Fig. 6a for $x_{Ti} = 0.02$). For $x_{Cr} = 0.02$, the B feature is absent at 300 K, but it appears at higher T (Fig. 6b) and its intensity soon becomes larger than that in $x_{Ti} = 0.02$.

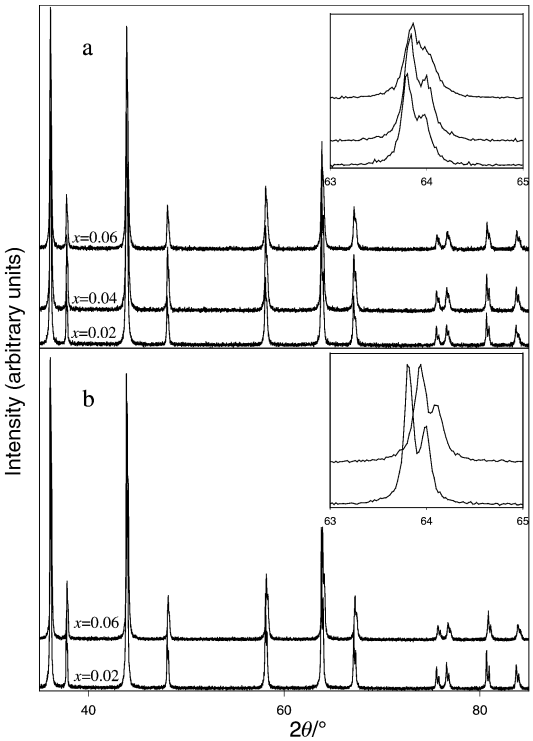

Fig. 1 X-Ray diffraction patterns for (a) Cr- and (b) Co-doped samples with different x content. Peak shift and broadening are evidenced in the inset.

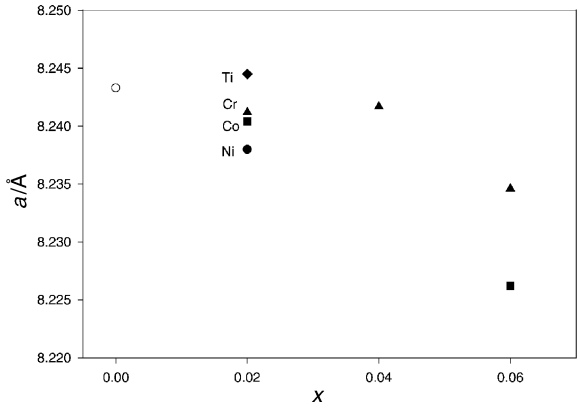

Fig. 2 Lattice parameter values as a function of x content for different doping ions.

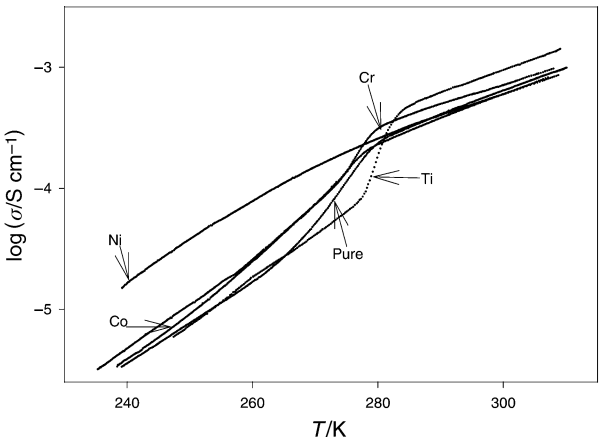

Fig. 3 Conductivity data of the $x = 0.02$ doped samples compared with the pure spinel.

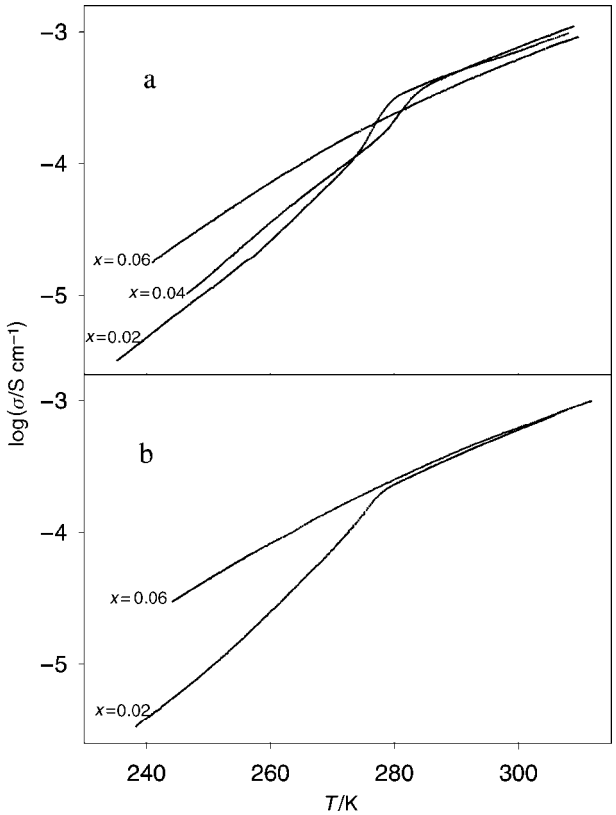

Fig. 4 Conductivity data of (a) Cr- and (b) Co-doped samples with different x content.

The $x_{Cr} = 0.04$, $x_{Cr} = 0.06$ and $x_{Ni} = 0.02$ samples have spectra similar to that of the undoped compound. Fig. 7 compares, for different temperatures, the spectra of the $x_{Ni} = 0.02$ (a) with those of the pure spinel (b).

In the $x_{Cr} = 0.02$, $x_{Ni} = 0.02$ and $x_{Co} = 0.06$ samples at 300 K, a sharp shoulder (C in Fig. 5) is seen at $g \approx 1.99$. It has been attributed to Mn^{4+} in Li_2MnO_3,[22] and is due to a very small fraction (<0.1%) of this phase present in these doped samples.

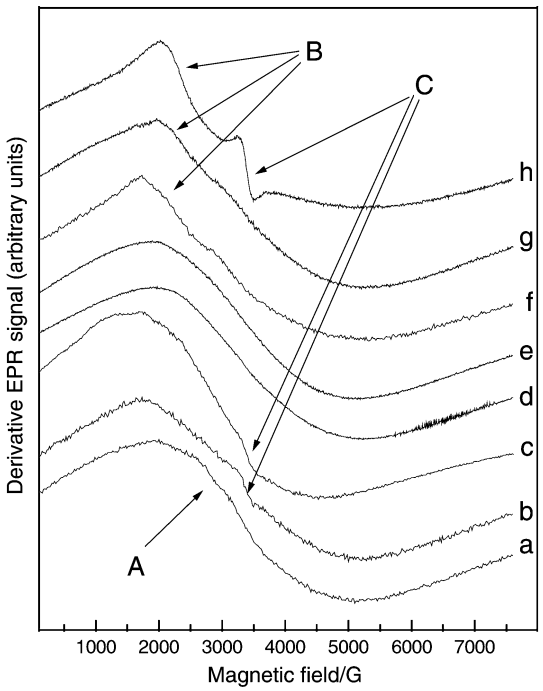

Fig. 5 EPR signals of the samples at 300 K: (a) pure spinel, (b) $x_{Ni} = 0.02$, (c) $x_{Cr} = 0.02$, (d) $x_{Cr} = 0.04$, (e) $x_{Cr} = 0.06$, (f) $x_{Ti} = 0.02$, (g) $x_{Co} = 0.02$, (h) $x_{Co} = 0.06$. Features A, B and C (see text) are evidenced.

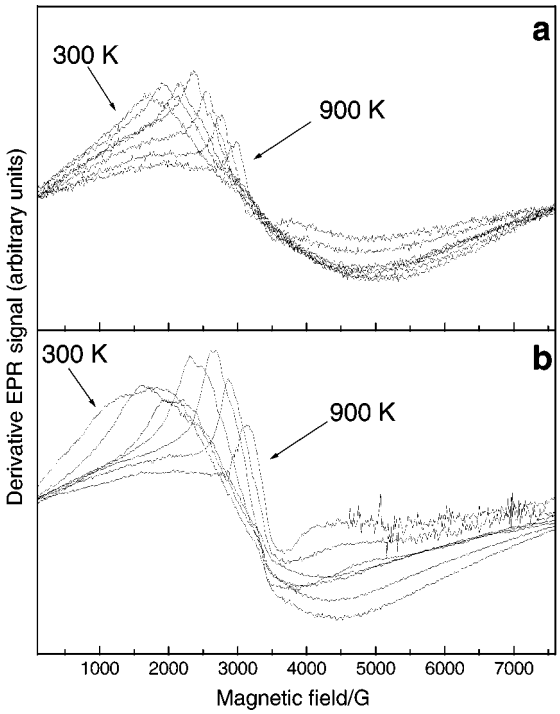

Fig. 6 EPR signals from 300 to 900 K in steps of 100 K of $x_{Ti} = 0.02$ (a) and of $x_{Cr} = 0.02$ (b) samples.

3.4. Static magnetic susceptibility

Static magnetic susceptibility (χ) yields information about the valence of the doping ion, which is related to changes in the slope of $1/\chi(T)$ in the paramagnetic region. The susceptibility is sensitive also to dilution of the dopant through the zero field cooled (ZFC) and field cooled (FC) separation temperature (T_0), as previously observed for Li-rich samples.[23]

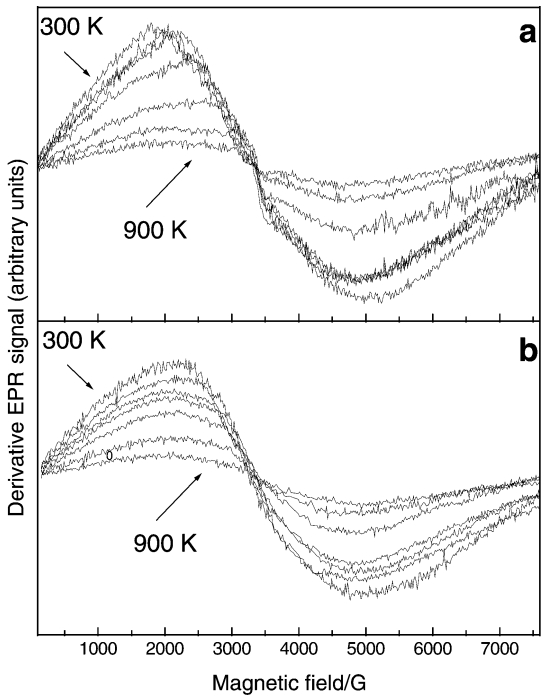

Fig. 7 EPR signals from 300 to 900 K in steps of 100 K of $x_{Ni} = 0.02$ (a) and of pure spinel (b).

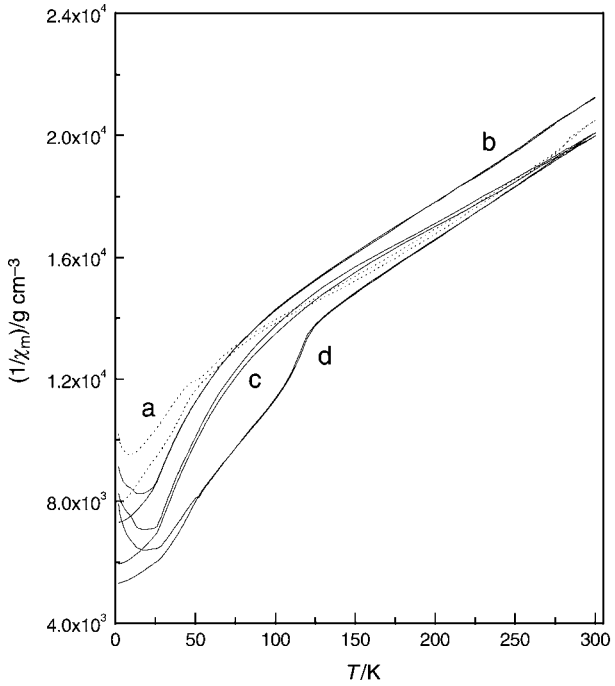

Fig. 8 $1/\chi_m(T)$ curves at $B = 1$ kG of: (a) pure spinel, (b) $x_{Cr} = 0.06$, (c) $x_{Co} = 0.06$, (d) $x_{Ni} = 0.02$ samples.

The behavior of $1/\chi(T)$ from 2 to 300 K for $x_{Cr} = 0.06$, $x_{Co} = 0.06$ and $x_{Ni} = 0.02$ samples is shown in Fig. 8, and compared with the trend of the pure spinel. The change in slope near 115 K in the $x_{Ni} = 0.02$ sample is believed to signal the presence of a small amount of MnO phase, which has an antiferromagnetic phase transition at 112–115 K.[24] This phase could not be detected by XRD.

4. Discussion

The EPR signal of lithium manganese spinel is due to Mn^{4+} ions and has been studied for $T < 500$ K.[22,25] As can be seen from Fig. 7b, it maintains a Lorentzian shape with a width of about 3000 G when the temperature is raised from 300 to 900 K while its intensity decreases according to the Boltzmann law. With the exception of Ti^{4+}, the doping ions in the octahedral sites are paramagnetic and contribute their own EPR signal.[26] However, for homogeneously substituted ions, this contribution cannot modify the Mn peak significantly because the interaction between different ions does not allow exchange narrowing, and broad signals result because of the dipolar interaction. The possible EPR signal of the doping ion should not be observed, contrary to what should happen for paramagnetic ions diluted in a diamagnetic matrix. So, the EPR signal of $x_{Cr} = 0.04$, $x_{Cr} = 0.06$ and $x_{Ni} = 0.02$ samples is essentially the same as that of the pure spinel, and has the same trend with temperature.

In the other samples we observe a feature (B) which is independent of doping ion and which changes dramatically with temperature. With increasing T, this feature approaches $g = 2$, narrows, and then its intensity decreases rapidly, according to a decreasing of the involved paramagnetic centres. This phenomenon may be associated with formation of Mn^{4+} clusters in low symmetry sites,[25] possibly at the boundaries of regions with different concentrations of the dopant. With increasing temperature, the intensity decreases because local distortions become smaller; this phenomenon is due to the flexibility of the octahedral coordination and the adaptability of the spinel lattice. As expected, the B feature is affected by the thermal treatment of the sample. In fact, we found that in the $x_{Cr} = 0.04$ sample the B feature is fully removed by additional grinding–annealing cycles. The removal by grinding–annealing is only partial for $x_{Co} = 0.06$, where a strong C-feature related to a Li_2MnO_3 phase is also observed (Fig. 9a and 9b). Thus, EPR spectra yield information about the homogeneous dilution of doping ions in the spinel matrix. On the other hand, X-ray measurements with the Co and Cr doped samples do not reveal significant differences in the patterns.

The susceptibility measurements give information about the oxidation state of the doping ions. We restrict the discussion to the samples in Fig. 8. The $x_{Ni} = 0.02$ sample shows a decrease in the average magnetic moment with respect to that of the pure spinel. This is due to the smaller value of the Ni^{2+} magnetic moment with respect to that of Mn^{3+} ($m_{Ni^{2+}} = 2.83$ μ_B and $m_{Mn^{3+}} = 4.9$ μ_B) and to the formation of Mn^{4+} ions for charge balance. The $m_{Mn^{4+}}$ value (3.87 μ_B) is lower than $m_{Mn^{3+}}$ and consistent with the larger temperature derivative of $1/\chi(T)$. The same holds true for the $x_{Cr} = 0.06$ sample, in which the Mn^{3+} ion is substituted by Cr^{3+} ($m_{Cr^{3+}} = 3.87$ μ_B). The $x_{Co} = 0.06$ sample shows a decreased temperature derivative of $1/\chi(T)$, as expected for a 3+ oxidation state ($m_{Co^{2+}} =$ 3.87–5 μ_B, $m_{Co^{3+}} = 4.9$–5.5 μ_B, higher than $m_{Mn^{3+}}$ due to the orbital contribution[27]). The displacement of T_0 to lower temperature, relative to the stoichiometric compound, is the largest in the $x_{Cr} = 0.06$ sample, due to the high amount of dopant and to the good homogeneity of doping.

The conductivity measurements in the Cr^{3+} and Co^{3+} doped samples display a progressive reduction, with increasing dopant, of $d\sigma/dT$ in the transition region. For $x_{Co} = 0.06$, $x_{Cr} = 0.06$ and $x_{Ni} = 0.02$ samples, no change in slope is observed. On the contrary, for $x_{Ti} = 0.02$ sample, the change of $d\sigma/dT$ is larger, and shifted towards higher temperatures, relative to the pure sample. This fact implies that Ti does not substitute the Jahn Teller ion (Mn^{3+}) and is therefore in the 4+ oxidation state. The above observations agree with the ideal substitutional model according to which the 16d site is a host for both lithium excess and the transition metal cations. The charge balance of the octahedral sites is achieved by a suitable change in the Mn^{3+} and Mn^{4+} amounts. For the Li-rich spinel, the charge distribution on the octahedral frame can be represented by: $[Li_y^{+}Mn_{1-3y}^{3+}Mn_{1+2y}^{4+}]_{octa}$. When a bivalent cation (Ni^{2+}) is substituted, we should consider the

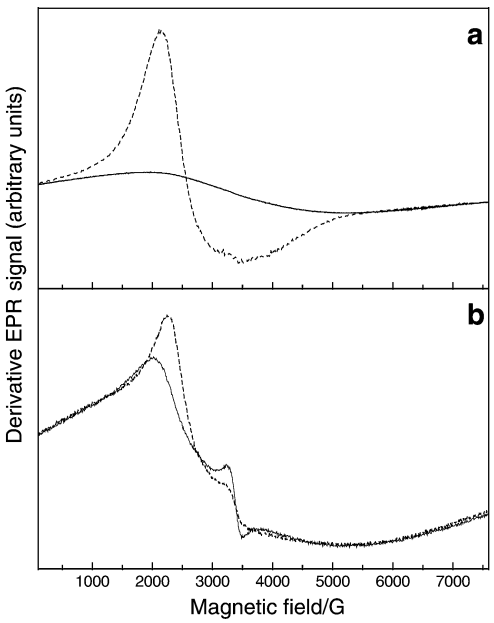

Fig. 9 EPR signal of: (a) $x_{Cr} = 0.04$ and (b) $x_{Co} = 0.06$ before (dashed lines) and after (solid lines) additional thermal annealing cycles.

charge distribution:

$$[Li_y^{+}Ni_x^{2+}Mn_{1-3y-2x}^{3+}Mn_{1+2y+x}^{4+}]_{octa}.$$

Here, $[Mn^{3+}]$ decreases faster than $[Mn^{4+}]$ increases. When trivalent cations (Cr^{3+}, Co^{3+}) are substituted, the charge distribution becomes:

$$[Li_y^{+}M_x^{3+}Mn_{1-3y-x}^{3+}Mn_{1+2y}^{4+}]_{octa}.$$

Here, we have a decrease in $[Mn^{3+}]$ with a constant $[Mn^{4+}]$ when the dopant is increased. Therefore, a suitable dopant concentration may remove the J–T distortion. On the other hand, the presence of $M = Ti^{4+}$ decreases $[Mn^{4+}]$ according to

$$[Li_y^{+}M_x^{4+}Mn_{1-3y}^{3+}Mn_{1+2y-x}^{4+}]_{octa},$$

This doping mechanism is not effective in removing the cooperative J–T effect.

The capability of a lattice to maintain the undistorted structure is determined by the ratio $r = [Mn^{4+}]/[Mn^{3+}]$. From the charge distributions discussed above and the fact that the J–T transition is suppressed for $x_{Ni} = 0.02$, $x_{Cr} = 0.06$ and $x_{Co} = 0.06$, we obtain $r \geqslant 1.18$ for the region of stability. This result agrees with the absence of the J–T transition in a Li-rich sample ($y = 0.035$, $x = 0$)[7] for which $r = 1.20$. On the other hand, the $x_{Ti} = 0.02$ sample, where the J–T distortion is not inhibited, has $r = 1.09$.

The application of the Rietveld method on the basis of the cubic spinel structural model (single-phase) gives satisfactory results notwithstanding the fact that an accurate investigation of dopant content and its substitution on the Mn site cannot be performed, due to the low difference in the X-ray scattering power between the atom types. The $x_{Ti} = 0.02$ sample shows a higher lattice parameter a, though not very much different from that of the pure sample (Fig. 2). Cr^{3+} and Co^{3+} have almost no effect, while the Ni^{2+} ion reduces the lattice parameter even at a 1% substitution, possibly because of stronger M–O bonds.[14] The observed increase in peak broadening in the XRD patterns with increasing Cr^{3+} (which is homogeneously distributed in the spinel, according to the EPR results) may be due to a decreased crystallite size (inset of Fig. 1). The peak broadening observed in the $x_{Co} = 0.06$ sample may be due to some gradient of concentration which is not cancelled even by repeated annealing.

5. Conclusions

This study shows that, among Ti^{4+}, Co^{3+}, Cr^{3+} and Ni^{2+} ions, only Cr^{3+} and Ni^{2+} form stable, undistorted and homogeneously distributed $[MO_6]$ octahedra when substituted in the spinel lattice. Cr and Ni improve the stability of the spinel and the electronic conductivity near r.t., both major requirements for electrochemical applications.[15,16] According to the literature,[17] the de-lithiation process is impaired in highly doped samples. This is why it is of practical interest to know the minimum x-value which prevents the J–T transition.

The complete removal of the J–T transition observed for $x_{Co^{3+}} = 0.06$, $x_{Cr^{3+}} = 0.06$ and for $x_{Ni^{2+}} = 0.02$ demonstrates that substitution of a small fraction of the Mn^{3+} J–T ion inhibits cooperative distortion. For all these samples, the ratio r is about 1.18 which can be considered as a limit value beyond which J–T cooperative distortion does not occur. For the $x_{Co} = 0.06$ sample, removal of the J–T effect may be partly due to the non-homogeneous distribution revealed by the EPR and XRD analyses. On the contrary, partial substitution of Mn by Ti^{4+} favors J–T structural distortion and does not improve the electrochemical performance. Note also that in $LiTi_{0.19}Mn_{1.81}O_4$ a local strain more than twice that in $LiM_{0.20}Mn_{1.80}O_4$ (M = Co, Cr) has been revealed.[18,19] X-Ray diffraction results are always consistent with a single cubic phase, and yield the lattice parameters with great accuracy. Finally, we have shown that the homogeneous distribution of the dopant, which is needed in an optimized Li–Mn cathode, can be probed by EPR and susceptibility measurements.

Acknowledgements

This work has been partially supported by "Consorzio per i Sistemi a Grande Interfase" (CSGI) and Istituto Nazionale di Coordinamento dei Materiali (MITER)

References

1 C. Julien, E. Haro-Poniatowski, M. A. Camacho-Lopez, L. Escobar Alarcon and J. Jimenez-Jarquin, *Mater. Sci-Eng. B*, 2000, **72**, 36.
2 P. Baurlein, R. Herr, M. Kloss, J. Kumpers, M. Maul and E. Meissner, *J. Power Sources*, 1999, **82**, 585.
3 J. Rodriguez Carvajal, G. Rousse, C. Masquelier and M. Hervieu, *Phys. Rev. Lett.*, 1998, **81**, 4660.
4 V. Massarotti, D. Capsoni, M. Bini, P. Scardi, M. Leoni, V. Baron and H. Berg, *J. Appl. Crystallogr.*, 1999, **32**, 1186.
5 V. Massarotti, D. Capsoni, M. Bini, G. Chiodelli, C.B. Azzoni and A. Paleari, *J. Solid State Chem.*, 1997, **131**, 94.
6 C. B. Azzoni, M. C. Mozzati, A. Paleari, V. Massarotti, M. Bini and D. Capsoni, *Z. Naturforsch. A*, 1998, **53**, 771.
7 A. Yamada, *J. Solid State Chem.*, 1996, **122**, 160.
8 C. B. Azzoni, M. C. Mozzati, A. Paleari, M. Bini, D. Capsoni, G. Chiodelli and V. Massarotti, *Z. Naturforsch. A*, 1999, **54**, 579.
9 J. M. Tarascon, E. Wang, F. Shokoohi, W. R. Mckinnon and S. Colson, *J. Electrochem. Soc.*, 1991, **138**, 2859.
10 R. J. Gummow, A. deKock and M. M. Thackeray, *Solid State Ionics*, 1994, **69**, 59.
11 K. Amine, H. Tukamoto, H. Yasuda and Y. Fujita, *J. Electrochem. Soc.*, 1996, **143**, 1607.
12 S. Kano and M. Sato, *Solid State Ionics*, 1995, **79**, 215.
13 L. Guohua, H. Hikuta, T. Uchida and M. Wakihara, *J. Electrochem. Soc.*, 1996, **143**, 178.
14 H. Berg, J. O. Thomas, W. Liu and G. C. Farrington, *Solid State Ionics*, 1998, **112**, 165.
15 B. Ammundsen, D. J. Jones, J. Roziere and F. Villain, *J. Phys. Chem. B*, 1998, **102**, 7939.
16 K. Oikawa, T. Kamiyama, F. Izumi, D. Nakazato, H. Ikuta and M. Wakihara, *J. Solid State Chem.*, 1999, **146**, 322.
17 P. Aitchison, B. Ammundsen, D. J. Jones, G. Burns and J. Roziere, *J. Mater. Chem.*, 1999, **9**, 3125.
18 L. Hernan, J. Morales, L. Sanchez and J. Santos, *Solid State Ionics*, 1999, **118**, 179.
19 A. D. Robertson, S. H. Lu, W. F. Averill and W. F. Howard, *J. Electrochem. Soc.*, 1997, **144**, 3500.
20 A. Antonini, C. Bellitto, M. Pasquali and G. Pistoia, *J. Electrochem. Soc.*, 1998, **145**, 2726.
21 J. Rodriguez-Carvajal, *Physica B*, 1993, **192**, 55.
22 V. Massarotti, D. Capsoni, M. Bini, C. B. Azzoni and A. Paleari, *J. Solid State Chem.*, 1997, **128**, 80.
23 P. Endres, B. Fuchs, S. Kemmler-Sack, K. Brandt, G. Faust-Becker and H. W. Praas, *Solid State Ionics*, 1996, **89**, 221.
24 D. J. Craik, *Magnetic Oxides*, Wiley, London, 1975, Part 1, p. 29.
25 R. Stoyanova, M. Gorova and E. Zhecheva, *J. Phys. Chem. Solids*, 2000, **61**, 609.
26 A. Abragam and B. Bleaney, in *Electron Paramagnetic Resonance of Transition Ions*, Clarendon, Oxford, 1970, p. 430.
27 D. H. Martin, *Magnetism in Solids*, Iliffe Books Ltd, London, 1967, p. 202.